Available online at www.sciencedirect.com
SCIENCE DIRECT®
ELSEVIER
Solid-State Electronics 47 (2003) 2245–2248
SOLID-STATE ELECTRONICS
www.elsevier.com/locate/sse

Nanoscale analysis of $YBa_2Cu_3O_{7-x}/La_{0.67}Ca_{0.33}MnO_3$ interfaces

Maria Varela [a,*], Andrew R. Lupini [a], Stephen J. Pennycook [a], Zouhair Sefrioui [b], Jacobo Santamaria [b]

[a] *Condensed Matter Sciences Division, Oak Ridge National Laboratory, Oak Ridge, TN 37831-6031, USA*
[b] *GFMC, Dpto. Física Aplicada III, Universidad Complutense de Madrid, 28040 Madrid, Spain*

Received 12 November 2002; accepted 12 April 2003

Abstract

The structure of interfaces in superconducting/ferromagnetic $YBa_2Cu_3O_{7-x}/La_{0.67}Ca_{0.33}MnO_3$ superlattices has been analyzed by scanning transmission electron microscopy and high spatial resolution electron energy loss spectroscopy. Individual layers are flat over long lateral distances. The interfaces are coherent, free of defects, exhibiting no roughness, and are located at the BaO plane of the superconductor. Concerning chemical disorder, EELS measurements show the absence of measurable chemical interdiffusion within experimental error bars.
© 2003 Elsevier Ltd. All rights reserved.

Keywords: Superlattices; Interfaces; Electron microscopy; High T_c superconductivity; Manganites

Ferromagnetic/superconducting (F/S) superlattices have attracted a lot of attention due to the possibility they offer of studying the interplay of superconductivity and magnetism [1–4]. Most of this work has been performed in metallic superlattices, however, in the last years much attention has been payed to oxide based F/S superlattices, combining a high critical temperature superconductor and a colossal magnetoresistant (CMR) oxide [5–7]. The different interaction phenomena that may occur, like proximity effects, coupling phenomena, charge transfer etc., will be directly influenced by the structure and specially by the physical and/or chemical disorder of the interfaces that separate them. Actually, CMR materials are charge transfer type oxides with carriers showing significant O 2p character [8], like the holes responsible for superconductivity in most high T_c superconducting compounds, and a variety of new phenomena could arise. Therefore, a direct structural characterization at the atomic scale of these interfaces is badly needed. In this work an atomically resolved structural and chemical characterization of interfaces in $YBa_2Cu_3O_{7-x}/La_{0.67}Ca_{0.33}MnO_3$ (YBCO/LCMO) superlattices by means of Z contrast imaging in a scanning transmission electron microscope is presented, together with a chemical characterization at the atomic scale carried out by high spatial resolution electron energy loss spectroscopy.

High quality YBCO/LCMO superlattices have been grown by high oxygen pressure sputtering (3.6 mbar) at 900 °C on $SrTiO_3$ substrates, beginning the deposition sequence with the LCMO layer [9]. This is a highly compatible system with a very low mismatch strain between YBCO and LCMO ($\varepsilon_a = a_{LCMO} - a_{YBCO}/a_{LCMO} = 0.5\%, \varepsilon_b = a_{LCMO} - b_{YBCO}/a_{LCMO} \leqslant 1\%$). Samples are magnetic and superconducting, with critical temperature and/or Curie temperature depending on the relative layer thicknesses [7]. X-ray diffraction spectra show well defined superlattice peaks denoting good sample quality [7]. Electron microscopy observations have been carried out in a VG HB501UX scanning transmission electron microscope (STEM), operated at 100 kV, and equipped with a field emission gun, a Nion aberration corrector

* Corresponding author.
E-mail address: mvarela@ornl.gov (M. Varela).

0038-1101/$ - see front matter © 2003 Elsevier Ltd. All rights reserved.
doi:10.1016/S0038-1101(03)00205-3

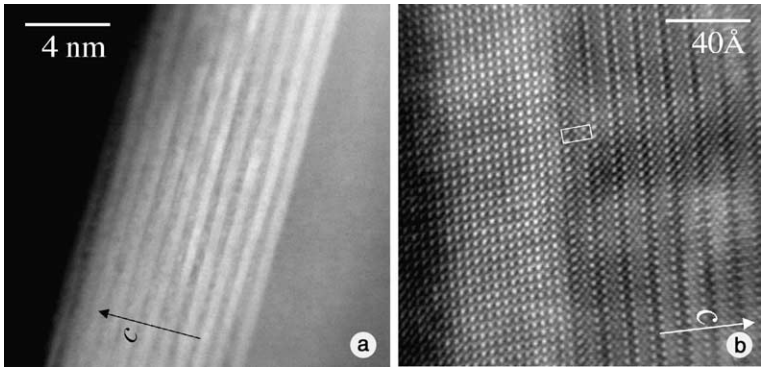

Fig. 1. (a) Low magnification Z contrast image of a [$YBCO_3/LCMO_{15}$] superlattice. (b) High resolution image of the YBCO/LCMO interface in a [$YBCO_8/LCMO_{15}$] sample. A YBCO unit cell has been marked with a white rectangle.

and a parallel electron energy loss spectrometer. This microscope can achieve a beam size and therefore a spatial resolution of 1.3 Å. Specimens for electron microscopy were prepared in cross section geometry by mechanical grinding, dimpling and finally ion milling with 4 kV Ar ions at an incidence angle of 7°. Final cleaning was done at low voltage of 2 kV.

Fig. 1(a) shows a low magnification image of a typical [$YBCO_{3\ u.c.}/LCMO_{15\ u.c.}$] superlattice, acquired with a high angle annular dark field detector (HAADF). The sample appears clean and free of defects, showing flat layers that are continuous over long lateral distances. Fig. 1(b) shows a high resolution image of the interface between YBCO and LCMO in a [$YBCO_{8\ u.c.}/LCMO_{15\ u.c.}$] superlattice. A YBCO unit cell has been marked for clarity. The interface is sharp and coherent, and shows a very good crystallinity. No dislocations or defects are observed. For this imaging technique, well known as Z-contrast, the intensity is roughly proportional to Z^2, giving direct compositional contrast [10]. The heavier the ion is, the brighter it appears on the image. In the YBCO structure the CuO chain plane is the lightest in the unit cell, and is further away the BaO plane than the CuO_2 layer. It therefore appears significantly darker in the image, while BaO planes show up with the brightest contrast. The CuO_2 planes can be observed sandwiched between them, together with the intermediate Y plane.

According to the interface structure observed in the images, a structural model of the interface can be suggested. As previously stated, the superlattice deposition sequence began by growing a LCMO layer on the $SrTiO_3$ substrate. This layer has been observed to show two different termination atomic planes, $La_{2/3}Ca_{1/3}$–O or Mn–O. Depending on which one occurs, two different interface structures can develop. Fig. 2 shows a typical example of an interface in with the terminating plane of LCMO is a $La_{2/3}Ca_{1/3}$–O plane. The interface can be accurately located through intensity traces as shown in Fig. 2(b). In this case the first atomic plane of the YBCO unit cell nucleating on top of the LCMO is constituted by the basal CuO chains plane, easily identifiable on the image due to its dark contrast. The structural model describing this configuration is shown on Fig. 2(c). However, the most common structure that was found by far was a MnO terminating plane, as shown in Fig. 3. In this case, the basal CuO chain plane is missing in the interface plane, and the YBCO growth begins with the BaO plane, as suggested in the adjacent structural model. Similar behaviour has already been reported for the deposition of Re-123 oxides on perovskites such as $SrTiO_3$ [11,12], where depending on the termination plane of the substrate, different stacking sequences would be observed in the first atomic layers. It is worth noting that the absence of CuO chains at the interface plane could have a serious impact on the superconducting properties of ultrathin YBCO layers sandwiched between LCMO layers.

Even though the interfaces have a very good crystallinity and roughness and/or steps are missing, there is another type of structural disorder that could deeply influence the properties of YBCO/LCMO heterostructures: chemical disorder or interdiffusion. Interface alloying could easily explain the presence of magnetic dead layers in the interface region [13,14] or the depression of superconductivity reported in ultrathin YBCO layers between LCMO spacers [7]. Magnetic impurities within the superconductor could cause pair breaking and lower the superconducting T_c value. A high spatial resolution compositional analysis can be achieved by measuring the changes in the intensity of EELS signal corresponding to the different chemical elements of interest across the interface. In this case, the changes in the La $M_{4,5}$ edge at 842 eV, Ba $M_{4,5}$ line at 781 eV and Mn $L_{2,3}$ edge at 644 eV were monitored by placing the electron beam at the interface and scanning across it. A summary of these data as a function of the distance to the interface is shown in Fig. 4(a). The intensities of the edges can be integrated and normalized to give a quan-

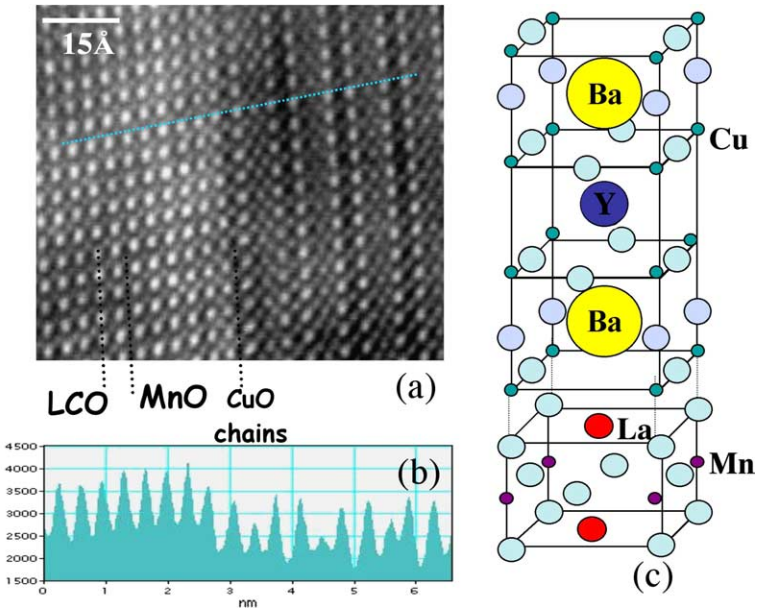

Fig. 2. (a) High resolution image of a LCMO/YBCO interface when the LCMO layer iterminates in a LaCa–O plane. A CuO chains plane is observed in the interface, that can be located through intensity traces as shown in (b). The adjacent picture (c) sketches a possible structural model of this interface.

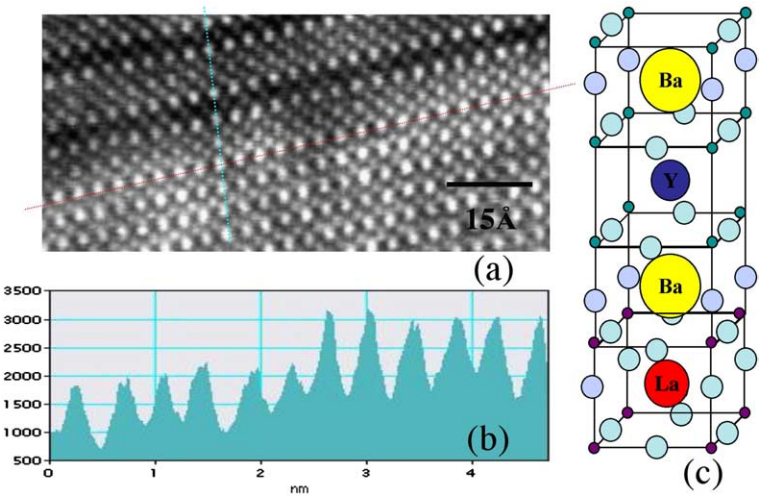

Fig. 3. (a) High resolution image of a LCMO/YBCO interface when the LCMO layer is terminated in a Mn–O plane. The interface has been marked with a dotted line for clarity. In this case the first atomic plane found in the YBCO layer is a BaO plane, as shown in the adjacent model (c).

titative measurement of elemental concentration. The concentration of Mn, La and Ba as a function of the distance to the interface is depicted in Fig. 4(b). Solid squares represent the Ba concentration, open circles correspond to the La, and solid circles represent the Mn signal. A sharp jump at the interface is observed, and even though the jump is not atomically sharp, the delay observed could probably be due to surface amorphous layers produced by the ion milling. From the observation of Fig. 4 it can be concluded that there is no major chemical intermixing of Ba ions into the LCMO layer, nor of Mn and/or La ions within the YBCO.

In conclusion, we have studied the structure of the interfaces in YBCO/LCMO superlattices. Interfaces are sharp and show good crystallinity. No defects or dislocations are observed. We did not find traces of chemical

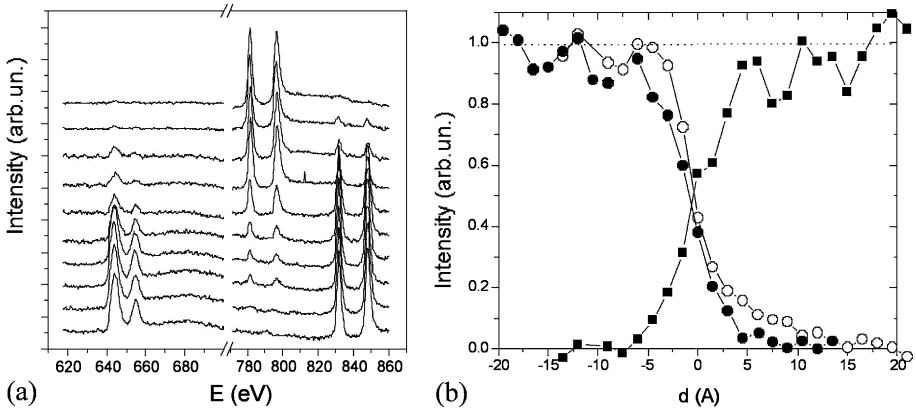

Fig. 4. (a) EEL spectra across the interface showing how the La $M_{4,5}$ edge (840 eV), Ba $M_{4,5}$ (781 eV) and Mn $L_{2,3}$ (642 eV) change across the interface. The spectra were acquired by successive jumps of 2 Å. (b) Integrated intensity, after normalization for La (open circles), Ba (solid squares) and Mn (solid circles) as a function of the distance to the interface.

disorder (interdiffusion) and/or alloying within experimental sensitivity. Within the two possible interface structures observed depending of the atomic termination of the LCMO layer, in most cases the interface is missing CuO chains in the YBCO layer. This feature should have a direct influence on the electronic properties, and should be taken into account when trying to explain the physical properties of ultrathin superconducting layers grown in such heterostructures.

Acknowledgements

Research performed as a Eugene P. Wigner Fellow and staff member (MV) at the Oak Ridge National Laboratory, managed by UT-Battelle, LLC, for the US Department of Energy under Contract DE-AC05-00OR22725. Financial support from CAM 07N/0008/2001 and Fundación Ramón Areces is acknowledged as well.

References

[1] Uher C, Clarke R, Zheng GG, Schuller IK. Interplay of superconductivity, magnetism and localization in Mo/Ni superlattices. Phys Rev B 1984;30(1):453–5.

[2] Aarts J, Geers JME, Brück E, Golubov AA, Coehoorn R. Interface transparency of superconductor/ferromagnetic multilayers. Phys Rev B 1997;56(5):2779–87.

[3] Kaneko S, Hiller U, Slaughter JM, Falco CM, Coccorese C, Maritato L. Superconducting transition temperatures and structure of MBE grown Nb/Pd multilayers. Phys Rev B 1998;58(13):8229–31.

[4] Verbanck G, Potter CD, Metlushko V, Schad R, Moschalkov VV, Bruynseraede Y. Coupling phenomena in superconducting Nb/Fe multilayer. Phys Rev B 1998; 57(10): 6029–35.

[5] Sá de Melo CAR. Magnetic exchange coupling through superconductors: a trilayer study. Phys Rev B 2000;62(18): 12303–16.

[6] Sá de Melo CAR. Magnetic exchange coupling in ferromagnet/Superconductor/Ferromagnet multilayers. Phys Rev Lett 1997;79(10):1933–6.

[7] Sefrioui Z, Varela M, Peña V, Arias D, Villegas JE, Saldarriaga W, et al. Supercondcutivity depression in ultrathin $YBa_2Cu_3O_{7-x}$ layers in $La_{0.7}Ca_{0.3}MnO_3/YBa_2Cu_3O_{7-x}$ superlattices. Appl Phys Lett 2002;81(24):4568–71.

[8] Ju HL, Sohn H-C, Krishnan KM. Evidence for O2p driven conductivity in $La_{1-x}Sr_xMnO_3$ ($0<x<0.7$) and $La_{0.7}Sr_{0.3}MnO_z$ thin films. Phys Rev Lett 1997;79(17):3230–3.

[9] Prieto P, Vivas P, Campillo G, Baca E, Castro LF, Varela M, et al. Magnetism and superconductivity in $La_{0.7}Ca_{0.3}MnO_3/YBa_2Cu_3O_7$ superlattices. J Appl Phys 2001;89(12): 8026–9.

[10] Pennycook SJ. Structure determination through *Z*-contrast microscopy. Adv Imaging Electron Phys 2002;123:173–205.

[11] Matijasevic VC, Ilge B, Staüble-Pümpin B, Rietveld G, Tuinstra F, Mooij JE. Nucleation of a complex oxide during epitaxial film growth: $SmBa_2Cu_3O_y$ on $SrTiO_3$. Phys Rev Lett 1996;76(25):4765–8.

[12] Staüble-Pümpin B, Matijasevic VC, Ilge B, Mooij JE, Peterse WJAM, Scholte PMLO, et al. Growth mechanisms of coevaporated $SmBa_2Cu_3O_y$ thin films. Phys Rev B 1995;52(10):7604–18.

[13] Sun JZ, Abraham DW, Rao RA, Eom CB. Thickness dependent magnetotransport in ultrathin manganite films. Appl Phys Lett 1999;74(20):3017–9.

[14] Bibes M, Balcells L, Valencia S, Fontcuberta J, Wojcik M, Jedryka E, et al. Nanoscale multiphase separation at $La_{2/3}Ca_{1/3}MnO_3/SrTiO_3$ interfaces. Phys Rev Lett 2001; 87(6):067210–3.